PHYSICAL REVIEW E **75**, 055203(R) (2007)

Quasipatterns in parametrically forced systems

A. M. Rucklidge
Department of Applied Mathematics, University of Leeds, Leeds LS2 9JT, United Kingdom

M. Silber
Department of Engineering Sciences and Applied Mathematics, Northwestern University, Evanston, Illinois 60208, USA

(Received 25 October 2006; published 4 May 2007)

We examine two mechanisms that have been put forward to explain the selection of quasipatterns in single- and multifrequency forced Faraday wave experiments. Both mechanisms can be used to generate stable quasipatterns in a parametrically forced partial differential equation that shares some characteristics of the Faraday wave experiment. One mechanism, which is robust and works with single-frequency forcing, does not select a specific quasipattern: we find, for two different forcing strengths, 12-fold and 14-fold quasipatterns. The second mechanism, which requires more delicate tuning, can be used to select particular angles between wavevectors in the quasipattern.

DOI: 10.1103/PhysRevE.75.055203 PACS number(s): 47.54.Bd, 47.20.Ky, 61.44.Br

I. INTRODUCTION

The Faraday wave experiment consists of a horizontal layer of fluid that develops standing waves on its surface as it is driven by vertical oscillation with amplitude exceeding a critical value; see [1,2] for surveys. Faraday wave experiments have repeatedly produced new patterns of behavior requiring new ideas for their explanation. An outstanding example of this was the discovery of *quasipatterns* in experiments with one frequency [3] and two commensurate frequencies [4]. Quasipatterns do not have translation order, but their spatial Fourier transforms have 8-, 10-, or 12-fold (or higher) rotational order.

Two mechanisms have been proposed for quasipattern formation, both building on ideas of Newell and Pomeau [5]. One applies to single-frequency forced Faraday waves [6] and has been tested experimentally [7]. Another was developed to explain the origin of the two length scales in superlattice patterns [8,9] found in two-frequency experiments [10]. The ideas have not been tested quantitatively, but have been used qualitatively to control quasipattern [1,11] and superlattice pattern [12] formation in two- and three-frequency experiments.

One aim of this paper is to demonstrate that both proposed mechanisms for quasipattern formation are viable. In order to claim convincingly that we understand the pattern selection process, we have designed a partial differential equation (PDE) and forcing functions that produce *a priori* the particular patterns of interest:

$$\frac{\partial U}{\partial t} = (\mu + i\omega)U + (\alpha + i\beta)\nabla^2 U + (\gamma + i\delta)\nabla^4 U + Q_1 U^2 + Q_2|U|^2 + C|U|^2 U + i\,\mathrm{Re}(U)f(t), \qquad (1)$$

where $f(t)$ is a real-valued forcing function with period 2π, the pattern $U(x,y,t)$ is a complex-valued function, $\mu<0$, ω, α, β, γ, and δ are real parameters, and Q_1, Q_2, and C are complex parameters. The PDE has multifrequency forcing and shares many of the characteristics of the real Faraday wave experiment, but has an easily controllable dispersion relation and simple nonlinear terms. In particular, the linear stability of the trivial solution reduces to the damped Mathieu equation, with subharmonic and harmonic tongues, the nonlinear terms allow three-wave interactions, and there is a Hamiltonian limit ($\mu=\alpha=\gamma=0$, $Q_2=-2\bar{Q}_1$, and $C=-\bar{C}$).

One issue, which we do not address here, is the distinction between true and approximate quasipatterns, as found in numerical experiments with periodic boundary conditions. Owing to the problem of small divisors, there is as yet no satisfactory mathematical treatment of quasipatterns. (This issue is discussed in detail in [13].) In spite of this, the stability calculations described below, which are in the framework of a 12-mode amplitude expansion truncated at cubic order, prove to be a reliable guide to finding parameter values where approximate quasipatterns are stable. The fact that stable 12-fold quasipatterns are found where expected demonstrates that this approach provides useful information.

With advances in computing power, we are able to go to larger domains and longer integration times to obtain very clean examples of approximate quasipatterns, going further than previous numerical studies [14]. In addition, we report here an example of a spontaneously formed 14-fold quasipattern.

II. PATTERN SELECTION

Resonant triads play a key role in the understanding of pattern selection mechanisms. Consider a two- (or more) frequency forcing function of the form

$$f(t) = f_m \cos(mt + \phi_m) + f_n \cos(nt + \phi_n) + \cdots, \qquad (2)$$

where m and n are integers, f_m and f_n are amplitudes, and ϕ_m and ϕ_n are phases. We consider m to be the dominant driving frequency, and focus on a pair of waves, each with wave number k_m satisfying the linear dispersion relation $\Omega(k_m) = m/2$. These waves have the correct natural frequency to be driven parametrically by the forcing $f(t)$. We write the critical modes in traveling wave form $z_1 e^{i\boldsymbol{k}_1\cdot\boldsymbol{x}+imt/2}$ and $z_2 e^{i\boldsymbol{k}_2\cdot\boldsymbol{x}+imt/2}$. These waves will interact nonlinearly with waves $z_3 e^{i\boldsymbol{k}_3\cdot\boldsymbol{x}+i\Omega(k_3)t}$, where $\boldsymbol{k}_3=\boldsymbol{k}_1+\boldsymbol{k}_2$ and $\Omega(k_3)$ is the frequency associated with k_3, provided that either (1) the same resonance condition is met with the temporal frequen-

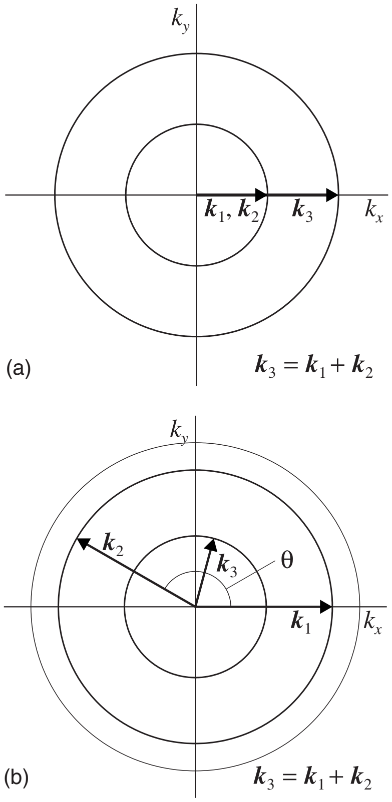

FIG. 1. (a) If the dispersion relation satisfies $\Omega(2k_m)=2\Omega(k_m)$, then two modes with wave number k_m and aligned wave vectors $\boldsymbol{k}_1=\boldsymbol{k}_2$ (inner circle) resonate in space and time with a mode with $\boldsymbol{k}_3=2\boldsymbol{k}_1$ (outer circle). (b) With two-frequency forcing, consider two modes with wave vectors $\boldsymbol{k}_1$ and $\boldsymbol{k}_2$, with the same wave number k_m, and with $\Omega(k_m)=m/2$ (middle circle). The nonlinear combination of these two waves can, in the presence of forcing at frequency n (outer circle), interact with a mode with wavevector $\boldsymbol{k}_3$ (inner circle), provided $\boldsymbol{k}_3=\boldsymbol{k}_1+\boldsymbol{k}_2$ and $\Omega(k_3)=|m-n|$.

cies i.e., $\Omega(k_3)=m/2+m/2$, or (2) any mismatch $\Delta=|\Omega(k_3)-m/2-m/2|$ in this temporal resonance condition can be compensated by the forcing $f(t)$. The first case corresponds to a 1:2 resonance, which occurs even for single-frequency forcing ($f_n=0$), and the second applies, e.g., to two-frequency forcing with the third wave oscillating at the difference frequency: $\Omega(k_3)=|m-n|$ and $\Delta=n$. Note that in both cases the temporal frequency $\Omega(k_3)$ determines the angle θ between the wave vectors $\boldsymbol{k}_1$ and $\boldsymbol{k}_2$ via the dispersion relation (Fig. 1), and therefore provides a possible selection mechanism for certain angles in the spatial Fourier spectrum being enhanced or suppressed. Selecting an angle of 0° [Fig. 1(a)] is a special case.

The nonlinear interactions of the modes can be understood by considering resonant triad equations describing small-amplitude patterns, which take the form

$$\dot{z}_1 = \lambda z_1 + q_1\bar{z}_2 z_3 + (a|z_1|^2 + b|z_2|^2)z_1 + \cdots ,$$

$$\dot{z}_2 = \lambda z_2 + q_1\bar{z}_1 z_3 + (a|z_2|^2 + b|z_1|^2)z_2 + \cdots ,$$

$$\dot{z}_3 = \lambda_3 z_3 + q_3 z_1 z_2 + \cdots , \qquad (3)$$

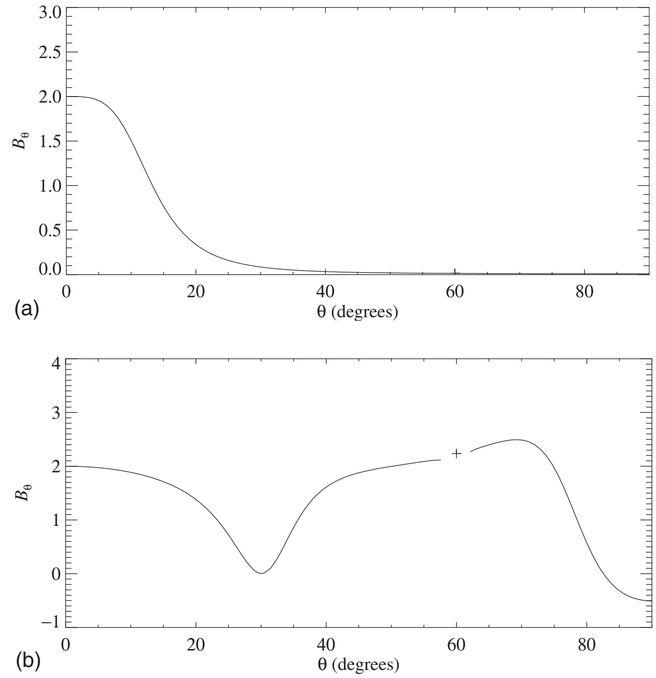

FIG. 2. B_θ for the two cases. (a) Single-frequency forcing with 1:2 resonance. The parameter values are $\omega=1/3$, $\beta=-1/6$, $\delta=0$, $\mu=-0.005$, $\alpha=0.001$, $\gamma=0$, $Q_1=3+4i$, $Q_2=-6+8i$, $C=-1+10i$, $m=1$, $\phi_1=0$, and $f_1=0.024\,002$. (b) Multifrequency (4, 5, 8) forcing, with $\omega=0.633\,975$, $\beta=-1.366\,025$, $\delta=0$, $\mu=-0.2$, $\alpha=-0.2$, $\gamma=-0.15$, $Q_1=1+i$, $Q_2=-2+2i$, $C=-1+10i$, $f_4=0.534\,37$, $f_5=0.763\,16$, $f_8=1.490\,63$, $\phi_4=0$, $\phi_5=0$, and $\phi_8=0$. The + symbol is the result of a separate calculation.

where all coefficients are real, and the dots refer to derivatives on time scales long compared to the forcing period. The quadratic coupling coefficients q_j are $O(1)$ in the forcing in the 1:2 resonance case, and $O(|f_n|)$ in the difference frequency case. For other angles θ between the wave vectors $\boldsymbol{k}_1$ and $\boldsymbol{k}_2$, we expect $q_j\approx 0$ because the temporal resonance condition for the triad of waves is not met. Here we are assuming that the z_3 mode is damped when λ goes through zero ($\lambda_3<0$), so z_3 can be eliminated via center manifold reduction near the bifurcation point ($z_3\approx q_3 z_1 z_2/|\lambda_3|$), resulting in the bifurcation problem

$$\dot{z}_1 = \lambda z_1 - (|z_1|^2 + B_\theta|z_2|^2)z_1,$$

$$\dot{z}_2 = \lambda z_2 - (|z_2|^2 + B_\theta|z_1|^2)z_2, \qquad (4)$$

where we have rescaled z_1 and z_2 by a factor of $1/\sqrt{|a|}$ and assumed that $a<0$. Here $B_\theta=b/a+q_1q_3/a|\lambda_3|$ includes the contribution from the slaved mode z_3, and depends on the angle θ between the two wave vectors $\boldsymbol{k}_1$ and $\boldsymbol{k}_2$.

The function B_θ has important consequences for the stability of regular patterns. Within the context of (4), stripes are stable if $B_\theta>1$, while rhombs associated with a given angle θ are preferred if $|B_\theta|<1$. By judicious choice of forcing frequencies, we have some ability to control the magnitude of B_θ over a range of angles θ [9], which allows the enhancement or suppression of certain combinations of wave vectors in the resulting patterns, depending on the sign of

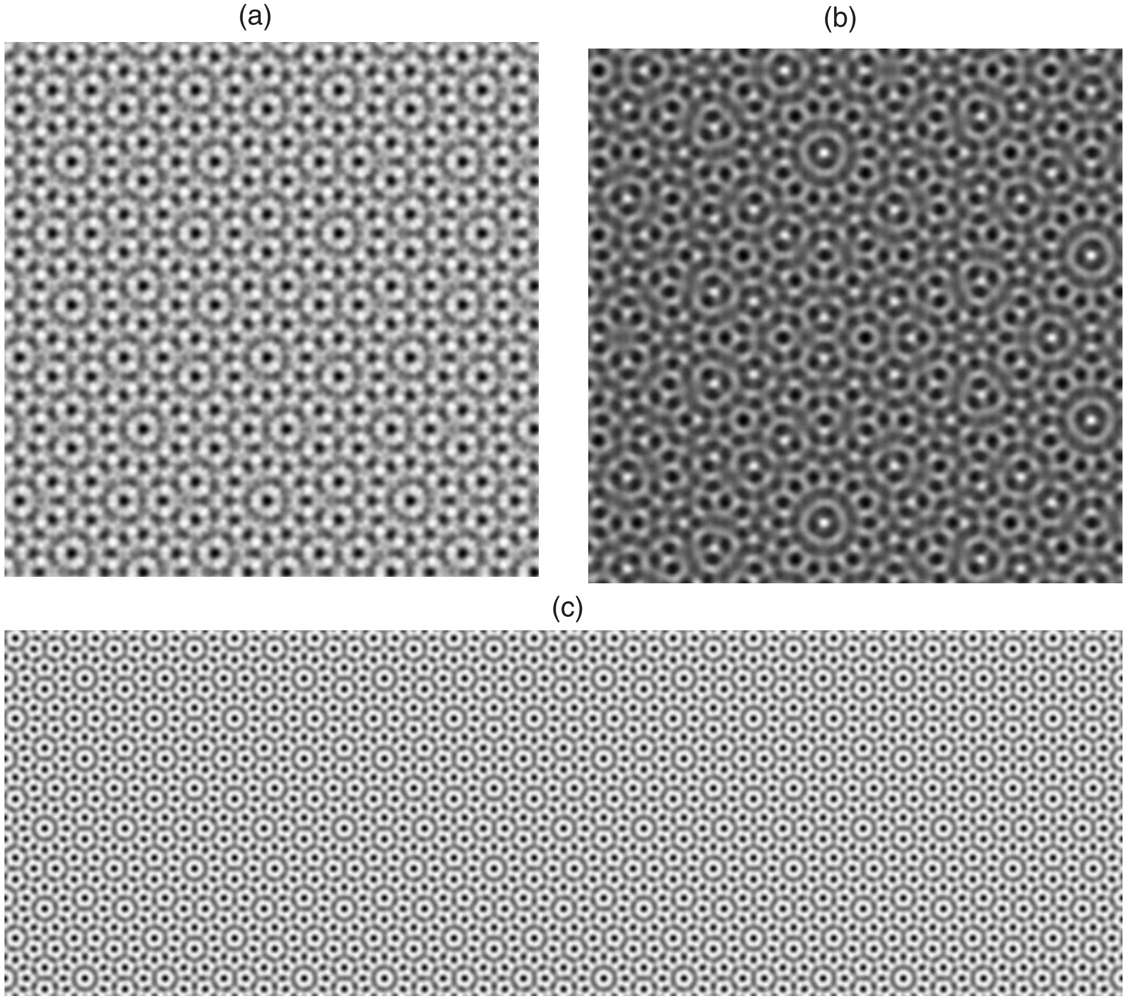

FIG. 3. (a) With parameter values as in Fig. 2(a), in a domain 30×30 wavelengths, and forced at 1.1 times the critical amplitude, we find a subharmonic 12-fold quasipattern. (b) At 1.3 times critical, the 12-fold quasipattern is unstable and is replaced by a 14-fold quasipattern. (c) With parameter values as in Fig. 2(b) and with (f_4,f_5,f_8) set at 1.003 times their critical values, we find a harmonic 12-fold quasipattern in a 112×112 domain (only a third is shown).

q_1q_3. Alternatively, if we choose forcing frequencies that select an angle of 0°, then this can lead to a large resonant contribution: a can become large [6]. This causes the rescaled cross-coupling coefficient B_θ to be small over a broad range of θ away from $\theta=0$. (As $\theta\to0$, it can be shown that $B_\theta\to2$.)

III. RESULTS

We present parameter values that demonstrate that the two mechanisms are viable methods of predicting parameter values for stable approximate quasipatterns.

The dispersion relation of the PDE (1) is $\Omega(k)=\omega-\beta k^2+\delta k^4$. With single-frequency forcing, we choose $m=1$, and a spatial scale so that modes with $k=1$ are driven subharmonically: $\Omega(1)=\frac{1}{2}$. To have 1:2 resonance in space and time, we impose $\Omega(2)=1$, which leads to $\omega=\frac{1}{3}+4\delta$ and $\beta=-\frac{1}{6}+5\delta$. We choose $\delta=0$, small values for the damping coefficients μ, α, and γ, and order one values for the nonlinear coefficients. We solve the linear stability problem numerically to find the critical value of the amplitude f_1 in the forcing function, and use weakly nonlinear theory [15] to calculate B_θ [Fig. 2(a)]. This curve has $B_0=2$, but B_θ drops away sharply, and is close to zero for $\theta\geqslant30°$, for the reasons explained above. We use B_θ at 30°, 60°, and 90° and find that, within the restrictions of a 12-mode expansion, 12-fold quasipatterns are stable.

A numerical solution of the PDE (1) forced at 1.1 times the critical value is shown in Fig. 3(a), in a square domain with periodic boundary conditions, of size 30×30 wavelengths, with 512^2 Fourier modes (dealiased). The gray scale corresponds to the real part of $U(x,y,t)$ at an integer multiple of the forcing period. The time-stepping method was the fourth-order ETDRK4 [16], with 20 timesteps per period of the forcing. The solution is an approximate quasipattern: the primary modes that make up the pattern are (30, 0) and (26, 15) and their reflections, in units of basic lattice vectors. These two wave vectors are 29.98° apart, and differ in length by 0.05%. The amplitudes of the modes differ by 0.5%. The initial condition was not in any invariant subspace, and the PDE was integrated for 160 000 periods of the forcing. However, when we increase the forcing to 1.3 times critical, we find that the 12-fold quasipattern is unstable and is replaced (after a transient of 50 000 periods) by an approximate 14-fold quasipattern [Fig. 3(b)]. In this case, the modes are (30, 0), (27, 13), (19, 23), and (7, 29), differing in length by 0.5% and having angles within 1.5° of 360°/14. The amplitudes differ by about 10%.

The second method of producing quasipatterns involves the weakly damped difference frequency mode, and is more selective, but also requires some fine-tuning of the parameters. In order to use triad interactions to encourage modes at 30°, we choose $m=4$, $n=5$ forcing, setting $\Omega(1)=2$, and requiring that a wave number involved in 30° mode interactions $(k^2=2-\sqrt{3})$ correspond to the difference frequency: $\Omega(k)=1$. One solution is $\omega=0.633\,975$, $\beta=-1.366\,025$, and $\delta=0$. Twelvefold quasipatterns also require modes at 90° to be favored, and for these choices of parameters $\Omega(\sqrt{2})$ is 3.37. Although this is not particularly close to 4, we can use 1:2 resonance (driving at frequency 8) to control the 90° interaction. The resulting B_θ curve [Fig. 2(b)] shows pronounced dips at 30° and 90° as required. Again, B_{30}, B_{60}, and B_{90} are used to show that, within a 12-amplitude cubic truncation, 12-fold quasipatterns are stable, this time between 0.9995 and 1.0095 times critical. Squares are also stable above 1.0015 times critical.

A numerical solution of the PDE (1) at 1.003 times critical is shown in Fig. 3(c), in a periodic domain 112×112 wavelengths (integrated using 1536^2 Fourier modes). This solution was followed for over 10 000 forcing periods. The larger domain allows an improved approximation to the quasipattern: the important wave vectors are (112, 0) and (97, 56), which are 29.9987° apart and differ in length by 0.004%. The amplitudes of these modes differ by 1%. A similar pattern was also found in a 30×30 domain, with the same modes as in Fig. 3(a).

IV. DISCUSSION

We investigated two quasipattern formation mechanisms for Faraday waves within a single PDE model of pattern formation via parametric forcing, and demonstrated viability of both mechanisms. One uses 1:2 resonance in space and time to magnify the self-interaction coefficient a and thereby, on rescaling, diminish the cross-coupling coefficient B_θ for angles greater than about 30°, which leads to "turbulent crystals" [5]. Within this framework, it is not clear why regular 8-, 10-, 12-, or 14-fold quasipatterns, or indeed any other combination of modes, should be preferred (although Zhang and Viñals [6] proposed that quasipatterns minimizing a Lyapunov function should be favoured). The mechanism is robust (the patterns are found well above onset), and requires only single-frequency forcing. A dispersion relation that supports 1:2 resonance in space and time is needed.

The existence of 14-fold (and higher) quasipatterns has been suggested before [6,13,17]; we have presented here a spontaneously formed 14-fold quasipattern that is a stable solution of a PDE. Examples where 14-fold symmetry is imposed externally have been reported in optical experiments [18]. The Fourier spectra of 12-fold and 14-fold quasipatterns are both dense, but those of 14-fold quasipatterns are much denser, owing to the difference between quadratic and cubic irrational numbers [13]. This difference may have profound consequences for their mathematical treatment.

The second mechanism uses three-wave interactions involving a damped mode associated with the difference of the two frequencies in the forcing to select a particular angle (30° in the example presented here). Using different primary frequencies, or altering the dispersion relation, allows other angles, or combinations of angles, to be selected. The advantage is that a forcing function can be designed to produce a particular pattern. On the other hand, the strongest control of B_θ occurs for parameters close to the bicritical point, which limits the range of validity of the weakly nonlinear theory used to compute stability. This issue will be pursued elsewhere.

ACKNOWLEDGMENTS

We are grateful for support from NSF (Grant No. DMS-0309667) and EPSRC (Grant No. GR/S45928/01). We are also grateful to Stéphan Fauve, Jay Fineberg, Ian Melbourne, Michael Proctor, Jeff Porter, Anne Skeldon, and Jorge Viñals for useful discussions, and we acknowledge the hospitality of the Isaac Newton Institute for Mathematical Sciences.

[1] H. Arbell and J. Fineberg, Phys. Rev. E **65**, 036224 (2002).
[2] A. Kudrolli and J. P. Gollub, Physica D **97**, 133 (1996).
[3] B. Christiansen, P. Alstrom, and M. T. Levinsen, Phys. Rev. Lett. **68**, 2157 (1992).
[4] W. S. Edwards and S. Fauve, J. Fluid Mech. **278**, 123 (1994).
[5] A. C. Newell and Y. Pomeau, J. Phys. A **26**, L429 (1993).
[6] W. B. Zhang and J. Viñals, Phys. Rev. E **53**, R4283 (1996).
[7] M. T. Westra, D. J. Binks, and W. Van de Water, J. Fluid Mech. **496**, 1 (2003).
[8] C. M. Topaz and M. Silber, Physica D **172**, 1 (2002).
[9] J. Porter, C. M. Topaz, and M. Silber, Phys. Rev. Lett. **93**, 034502 (2004).
[10] A. Kudrolli, B. Pier, and J. P. Gollub, Physica D **123**, 99 (1998).
[11] Y. Ding and P. Umbanhowar, Phys. Rev. E **73**, 046305 (2006).
[12] T. Epstein and J. Fineberg, Phys. Rev. E **73**, 055302(R) (2006).
[13] A. M. Rucklidge and W. J. Rucklidge, Physica D **178**, 62 (2003).
[14] W. B. Zhang and J. Viñals, Physica D **116**, 225 (1998).
[15] M. Silber, C. M. Topaz, and A. C. Skeldon, Physica D **143**, 205 (2000).
[16] S. M. Cox and P. C. Matthews, J. Comput. Phys. **176**, 430 (2002).
[17] C. M. Topaz, J. Porter, and M. Silber, Phys. Rev. E **70**, 066206 (2004).
[18] E. Pampaloni, P. L. Ramazza, S. Residori, and F. T. Arecchi, Phys. Rev. Lett. **74**, 3305 (1995).